Chapter IX, Section g

Methods for studying radiation-induced acute intestinal damage and regeneration in mice

Brian Leibowitz[1], Liang Wei[1], Xinwei Wang[1], Jian Yu[1]*

[1]Department of Pathology, [1]University of Pittsburgh Cancer Institute, University School of Medicine, Pittsburgh, PA, USA.

Correspondence:
Jian Yu, Ph.D., Hillman Cancer Center Research Pavilion, Suite 2.26h, 5117 Centre Ave, Pittsburgh, PA 15213. Email: yuj2@upmc.edu; Phone: 412-623-7786; Fax: 412-623-7778

Figures, 17, embedded
References: 56

Acknowledgements: Methods and Illustrations are solely for technical and educational purposes, and compiled from work in YU group for over ten years with contributions from many talented individuals who are not all listed as co-authors. Published work was cited in Figure legends and relevant text whenever possible, which provides a much more comprehensive context and details of chosen examples to the method chapter. The work in Yu lab has been support in part by NIH grants U19A1068021, U01DK085570, R01CA106348, and grants from American Society of Cancer (ACS), Flight Attendant Medical Institute (FAMRI) and Alliance for Cancer Gene Therapy (ACGT).

Introduction

Intestinal epithelium and intestinal stem cells

The adult small and large intestines are covered by a single layer of columnar epithelial cells with several vital functions, such as nutrient and water absorption as well as barrier. The intestinal epithelium is the fastest renewing tissue in an adult mammal with a renewal cycle estimated to be 3-5 days in mice, and driven by intestinal stem cells (ISCs) located in the crypts (Barker et al., 2008; Bjerknes and Cheng, 2005; Marshman et al., 2002). The intense proliferation is confined to the lower part of the crypts, and fuels this rapid epithelial turnover by producing transit amplifying cells and, subsequently, four major differentiated epithelial cell types including absorptive enterocytes, secretory goblet cells, enteroendocrine cells and Paneth cells. These differentiated cells are generally well-defined by morphology and markers produced (Barker et al., 2012; Bjerknes and Cheng, 1999; Winton and Ponder, 1990). Deep crypt secretory cells (Rothenberg et al., 2012) may represent the colon counterparts of Paneth cells. The gastrointestinal (GI) tract contains and interacts with 80% of the host immune system and microorganisms that outnumber host cells by a factor of ten, which are believed to regulate intestinal function, injury and regeneration in important ways that are far from clear (Yu, 2013).

Studies in the 1970s and 1980s defined two major populations of ISCs based on their locations: the stem cell zone model proposed by Cheng and Leblond defined the crypt base columnar cells (CBCs) sandwiched between Paneth cells (Bjerknes and Cheng, 1999, 2005), and the +4 label retaining cells (LRC) proposed by Potten and colleagues appeared radiosensitive (Potten et al., 1997). Work in the last ten years using mouse genetic models, particularly reporter mice, have led to major advances in the intestinal stem cell field (Barker et al., 2012) with the discovery of intestinal stem cell markers. ISCs include cycling and more quiescent stem cells in close proximity, while other cells such as Paneth cells and unidentified stromal cells define a niche critical for ISC maintenance and self-renewal. ISC markers described include Lgr5 (+) (Barker et al., 2007), Bmi1 (+) (Sangiorgi and Capecchi, 2008), mTert (+) (Montgomery et al., 2011), Hopx (+) (Takeda et al., 2011), Lrig1(+) (Powell et al., 2012; Wong et al., 2012), CD133 (Snippert et al., 2009; Zhu et al., 2009), Musashi-1 (Potten et al., 2003), or dye-exclusion (side population, SP) (Dekaney et al., 2005). Their inter-relationships and overlaps during homeostasis are not well-understood, and even less so during injury and recovery (Barker et al., 2012).

The successful culture of isolated crypts and ISCs (Sato et al., 2009) in so called enteroid (38) or organoid assays provides a very powerful tool to study crypt or ISC-intrinsic mechanisms. Tracing experiments indicated that the Lgr5 (+) stem-cell hierarchy is maintained in enteroids containing four major differentiated epithelial lineages. This "*in vitro*" clonogenic assay is expected to greatly help the understanding of stem cell injury and regeneration regulated by cell autonomous mechanisms, and certainly can be adapted to include niche components as discussed later.

Intestinal response to radiation in mice

Radiation causes double strand breaks which can be converted into other forms of DNA lesions upon replication, such as stalled forks, single strand breaks and aberrant chromosomal structures or segregation (Harper and Elledge, 2007). Accumulation of DNA damage is exacerbated upon rapid proliferation during crypt regeneration, and deficiency in various DNA repair proteins, *p21*, or *p53*, leading to non-apoptotic cell death (Leibowitz et al., 2011; Potten, 2004; Wei et al., 2016; Yu, 2013). Rapid renewal of the intestinal epithelium renders it susceptible to radiation-induced injury. Mouse models have been extensively used to study radiation-induced intestinal injury and regeneration. Under homeostatic conditions, the intestinal epithelium is a highly organized structure with a well-localized stem cell zone, progenitor cells and differentiated cells. Radiation induces rapid apoptosis of stem and TA cells. Interestingly, some cells at the +4 and TA region are sensitive to even 1 Gy with little consequence. Accumulating evidence indicates that the damage to the stem cell compartment by high dose radiation, i.e. greater than 14 Gy, leads to acute and lethal intestinal injury, referred to as the GI syndrome, which is unable to be rescued by bone marrow transplantation (Potten, 2004; Terry and Travis, 1989). Recent work has established the Lgr5 cells as a key target in this response (Metcalfe et al., 2014; Wang et al., 2015; Wei et al., 2016).

The rapid renewal, highly organized tissue structure and differential radio-sensitivity of epithelial cell types, close interaction with various BM-derived and stromal cell types, availability of genetic modified including conditional mouse models, similarity with the human intestinal system, and well-established yet still poorly understood cell-type specific DNA damage response in adult stem cells (Mandal et al., 2011), make the mouse small intestine a powerful model to study radiation-induced acute injury and recovery as well as intestinal stem cell biology. Given the complexity of the cell types within the intestinal epithelium and stroma and injury-induced spatial and temporal changes (i.e. loss, recruitment, homing, proliferation), staining-based methods (protein, RNA, lineage markers) are much more extensively used compared to molecular analysis using whole tissue or isolated cell types. Emerging evidence suggests that chronic intestinal damage is likely consequential to early toxicity (Hauer-Jensen et al., 2014) while the functional decline of the stem cell pool is not immediately apparent (Yu, 2013). Given the increasingly recognized role of gut epithelium in health and disease at the organismal level, there is a great need and interest to understand the nature of intestinal stem cell injury, and develop countermeasures to prevent or mitigate acute and delayed gut dysfunctions during accidental or medical exposures to radiation (Berbee and Hauer-Jensen, 2012; Greenberger, 2009; Yu, 2013).

This chapter will focus on basic models and methods assessing radiation-induced acute intestinal injury, including animal survival, GI structure damage, cell death, proliferation, DNA damage response, differentiation and function, as well as stem cell specific analysis using mice and the *in vitro* 3D culture system (Sato et al., 2009). Many of the same methods are also applicable to radiation-induced chronic injury.

Section 1. Radiation induced GI injury and recovery in mice

1.1 Study design and approval

All animal studies require institutional review and approval by the Institutional Animal Care and Use Committee. High dose radiation exposure is expected to result in rapid animal death, it is

recommended to carefully consider the endpoints as well as measures to reduce pain and suffering when developing such protocols. One also needs to be aware of strain and anatomic location differences in whole animal and intestinal specific radiation sensitivity and response.

1.2 Radiation models and survival analysis

1.2.1 Total body irradiation (TBI)

Radiation is known to cause dose-related and tissue-specific lethality (Potten, 2004). At higher doses with single exposure (i.e. 14 -18 Gy), TBI models cause lethal GI injury and the GI syndrome within 7-10 days. These models yield highly reproducible lethality, and structural, histological and marker changes in the intestinal epithelium and crypts within the first 96 hours. Mice were irradiated at the indicated dose (i.e. 15 Gy) at a rate of 76 cGy/min in a ^{137}Cs irradiator (Mark I; JL Shepherd and Associates, San Fernando, CA, USA), and followed for survival. 20% loss in body weight is acceptable when fatality is not accepted. Small intestines were harvested for histology and other molecular analysis. LC50s at 7 or 10 days have been used to assess the effects of compound, treatment, or genotype on radiation-induced GI injury.

1.2.2 Abdominal irradiation (ABI)

The ABI model is often used in survival studies to rule out a significant contribution of BM failure as the cause of death, the bone marrow is largely spared. ABI can be administered in the form of X-rays with a clinical grade linear accelerator (Varian Medical Systems, Palo Alto, CA). A 3-cm wide radiation band was used to deliver the required doses at a rate of 600 Monitor Units (146 cGy)/min to anesthetized animals in groups of 10-15 per run (Leibowitz et al., 2014b). The survival of the mice is comparable to TBI (Cs137) at 14.5 Gy and 15 Gy in our experience (Leibowitz et al., 2014b; Wang et al., 2015; Wei et al., 2016). Other investigators used subtotal body models (Kirsch et al., 2010; Potten, 2004) with varying degrees of BM shielding from the head to one extremity ,where the data on survival is somewhat variable perhaps related to the degree of shielding. Due to uneven tissue damage, none-TBI models generally preclude tissue, histological or molecular analysis.

1.2.3 Bone marrow transplantation

Bone marrow transplantation (BMT) can be used to dissect the role of BM, hematopoietic stem cells or other populations, and the homing of the BM cells in GI injury or recovery in radiation models (Leibowitz et al., 2014b). Lethal bone marrow failure occurs at lower doses with animal death around two weeks without BMT. Seven- to 9-week old female C57/B6 mice (The Jackson laboratory) received 10 Gy total body irradiation (TBI) the day prior to transplantation. The following morning, ~1 x 10^6 cells (whole marrow or $CD45^+$) from 7-9 week old male C57/B6 donors (with or without a GFP transgene) were transplanted intravenously via tail vein injection (Yu et al., 2010). Following transplantation, mice were allowed eight weeks for engraftment, at which time they were irradiated a second time and followed for survival or harvested at multiple time points for tissue analysis on intestine (host) and BM-reconstituted populations (Leibowitz et al., 2014b).

Figure 1. Survival curves using BMT, ABI and TBI models (Leibowitz et al., 2014b; Wei et al., 2016).

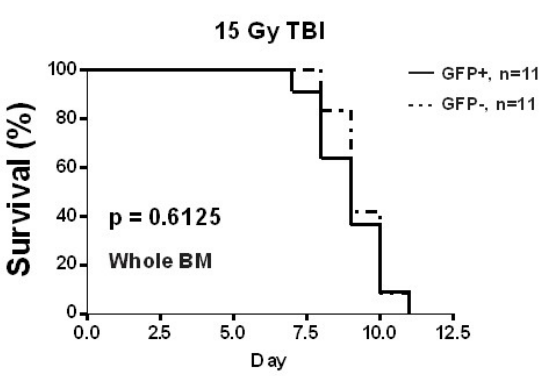

BMT on TBI-induced lethality

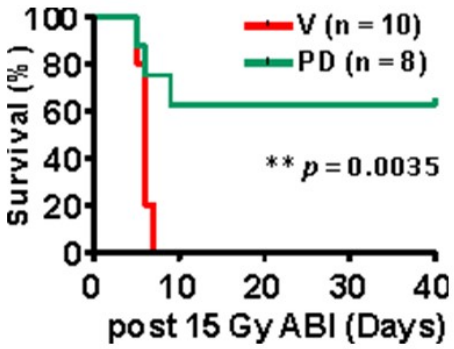

A CDK4/6 inhibitor reduces ABI-induced lethality

Section 2. Intestinal tissue preparation and structural analysis

2.1 Tissue harvest and preparation

Intestinal tissues are subject to rapid autolysis upon animal demise. The dedicated structure is best preserved by gentle handling and rapid fixation, followed by embedding in paraffin blocks. Fast and good fixation of samples prevents delicate villi from being damaged by residual gut digestive enzymes. It is recommended to cut the intestine into 10 or 20 cm segments for easier handling. If proliferation (S-phase entry) analysis is desired, mice can be injected i.p. with 100 mg/kg of BrdU (Cat# 858811, Sigma-Aldrich) two hours before sacrifice. Frozen blocks are used under specific conditions, but generally do not preserve the structures or the integrity of protein or RNA well enough. Due to the differences in structure and function and radiosensitivity based on the anatomic locations, it is critical to compare the same portion of intestine in any analysis.

2.3 Bundles and Swiss rolls

Immediately after the animal was euthanized, the middle section of jejunum (about 10 cm in length) was removed and carefully rinsed with ice-cold physiological saline (0.9% NaCl in water) using a 10 ml syringe with a blunted 18-guage needle (dulled so as to not damage internal mucosa). The tissue was cut into 1 cm pieces, and 6-8 pieces were bundled with 3M micropore tape and fixed immediately in a 20-fold volume of 10% neutral buffered formalin for overnight. The intestinal bundles were transferred to 70% ethanol and embedded in paraffin and sectioned (Qiu et al., 2008). One can also make “Swiss rolls” by opening the intestine longitudinally and tacking to a foam board during fixing, after which the tissue is rolled up and fastened in position with 3M micropore tape (Qiu et al., 2009a). Tissue sections following staining are used to assess structural features or damage, regeneration, and stem cell specific measures. These different preparations facilitate analysis across the circumference, entire length or unit length of the intestine, which can be critical when numbers of surviving crypts are significantly altered by

radiation or treatment. Usually 3-5 mice are used in each group, while multiple intestinal sections are scored in each animal.

Figure 2. Intestinal "bundles" or "Swiss Rolls" yield well-orientated cross or longitudinal sections (Leibowitz B and Yu J, unpublished)

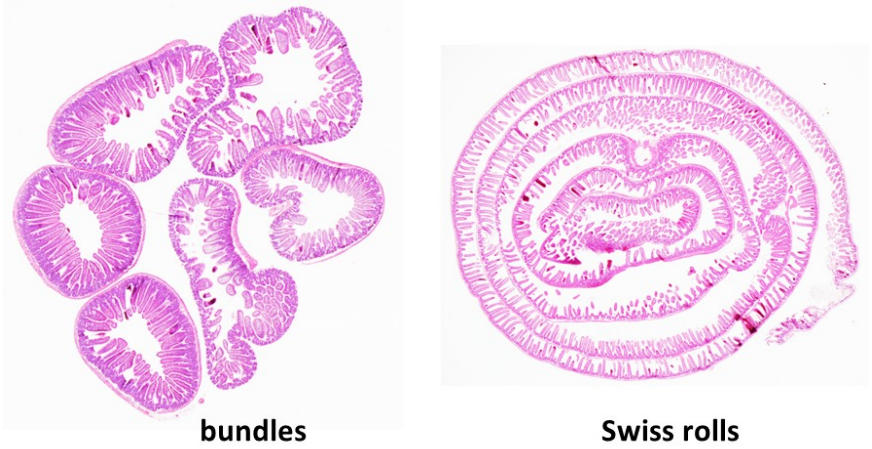

2.3 Intestinal Structure

2.3.1 Crypt and villus measurements

Histological analysis was performed following hematoxylin and eosin (H&E) staining to assess intestinal structure. Average villus and crypt size measurements were made using H&E sections using 100X images and SPOT 5.1 Advanced software (Diagnostic Instruments, Inc., Sterling Heights, MI) (Leibowitz et al., 2014b). Villus height measurements are based on 50-80 villi from different locations of the jejunum from three mice per group using SPOT 5.1 Advanced software (Leibowitz et al., 2014b) or ImageJ 1.46 software (National Institutes of Health, USA) (Wei et al., 2016). Crypt numbers are enumerated based on 3-5 full cross sections from three mice per group.

Figure 3. TBI- induced loss of crypts and shortening of villi are reduced by a CDK4/6 inhibitor (Wei et al., 2016). The surviving crypts and villus height were scored using H&E sections.

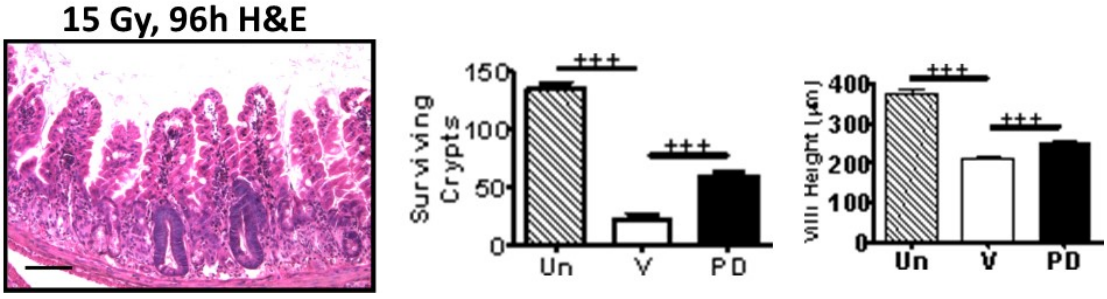

2.3.2 Crypt microcolony assay

The crypt microcolony assay is commonly used to quantify stem cell survival by counting regenerated crypts in H&E stained cross sections four days post-irradiation (Qiu et al., 2008; Roberts and Potten, 1994; Withers and Elkind, 1969). Surviving crypts are defined as containing five or more adjacent chromophilic, non-Paneth cells, at least one Paneth cell and a lumen. The number of surviving crypts was counted in 6-8 circumferences per mouse, with each approximately one cm apart. BrdU staining (see later) is also used to quantify regenerated crypts. The regenerated crypts contained 5 or more BrdU positive cells with a lumen, and appeared much enlarged compared to unirradiated controls. At least three mice are used in each group and the data from BrdU staining are reported as means ± standard deviation (s.d.).

Figure 4. Regenerated crypts after 15 Gy TBI at 96 hours visualized by H&E or BrdU staining are similar (Qiu et al., 2008).

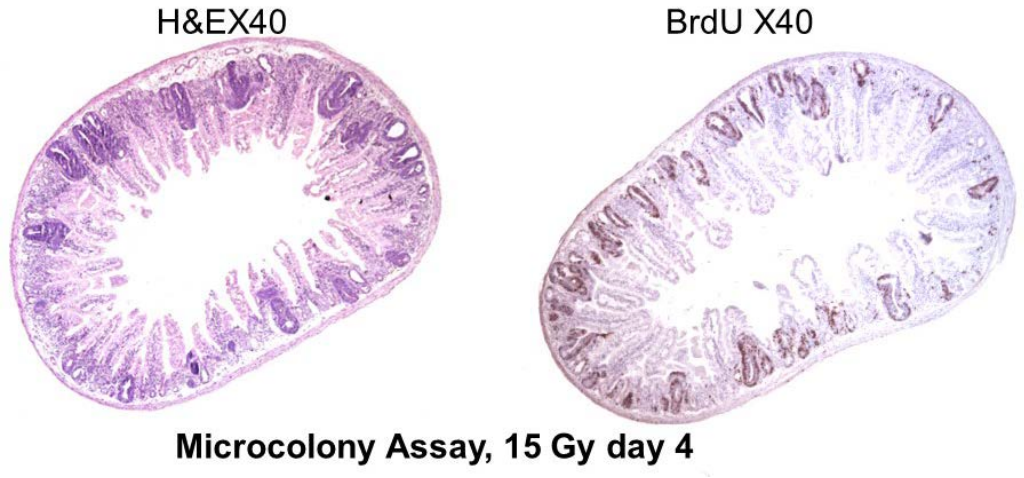

Section 3. Staining-based Tissue Analysis

A battery of well-characterized intestinal function or injury markers can be assessed by Immunohistochemistry (IHC) and immunofluorescence (IF), including those on apoptosis, non-apoptoic cell death, proliferation (limited to the crypts), differentiation, barrier, DNA damage response, and intestinal stem cells (discussed separated). Immunodetection of various proteins and markers was performed following deparaffinization and rehydrated through graded ethanols, and 3% hydrogen peroxide treatment (for IHC). For most markers, the choice of IF or IHC is based on the needs and practical concerns, such as whether or not co-staining is required, long-term preservation of signals or structural information is desired. Antigen retrieval is performed by boiling the sections for 10 minutes in 0.1 M citrate buffer (pH 6.0) with 1 mM EDTA. Non-specific antibody binding was blocked using the indicated serum. Usually 3-5 mice are used in each group in TBI models, while multiple intestinal sections are scored in each animal.

3.1 Cell death and proliferation

TUNEL IF. TUNEL staining identifies broken DNA ends and dying cells of apoptotic and non-apoptotic natures in the crypts after TBI (Leibowitz et al., 2011; Qiu et al., 2008). TUNEL staining was performed using an ApopTag Kit (Chemicon International, Temecula, CA) according to the manufacturer's instructions. The apoptotic index is scored in full longitudinal

sections of crypts containing at least 17 cells, including Paneth cells. The frequency of apoptosis for each cell position from the crypt bottom was scored in 200 half crypt sections and reported as mean ± SD.

Cleaved caspase-3 IHC. Cleaved caspase-3 identifies apoptotic cells, but not non-apoptotic cells or those dying from mitotic crisis in the crypts after TBI (Leibowitz et al., 2011; Qiu et al., 2008). Non-specific antibody binding was blocked using 20% goat serum at room temperature for 30 minutes. Sections were incubated overnight at 4°C in a humidified chamber with 1:100 diluted rabbit-anti-caspase-3 (cleaved, Asp 175) (9661; Cell Signaling Technologies, Beverly, MA). Sections were then incubated for 1 h at room temperature with biotinylated goat-anti-rabbit secondary antibodies (#31822; Pierce) and developed with an ABC kit and DAB (Vector Laboratories, Burlingame, CA).

BrdU IHC. BrdU staining is used for assess cell proliferation after pulse, i.e. for a few hours, or after chase (i.e. after a few days). Sections were deparaffinized and treated with proteinase K (20 μg/ml) for 20 min at 37°C, followed by 3% H_2O_2 for 5 min at room temperature. The staining was carried out following a standard protocol with an anti-BrdU antibody (1:100 in 10% goat serum, Invitrogen), secondary antibody (goat-anti-mouse-HRP, 1:100; Pierce) and developed by DAB (Vector laboratories, Burlingame, CA). BrdU-positive cells were counted in high-power (400X) fields, and the percentage of the BrdU-positive cells in total crypts was determined by counting 100 intact crypts and reported as mean ± SD.

Figure 5. Crypt apoptosis and proliferation analyzed by TUNEL, Cleaved Caspase-3 and BrdU staining 4 hours after 15 Gy TBI. Little or none was detected in the villus epithelium. (Leibowitz et al., 2014b; Wei et al., 2016)

Ki67 IF. Ki-67 staining is used to assess proliferation mostly in the TA zone (or above +4) (Qiu et al., 2009b; Qiu et al., 2013). Non-specific antibody binding was blocked 20% goat serum for

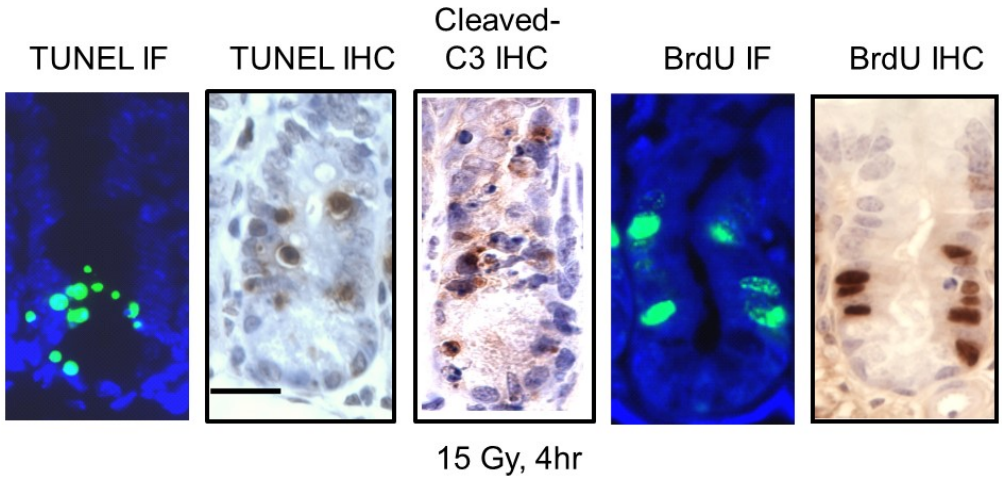

30 minutes at RT. The sections were incubated with rat anti-Ki67 antibody (DAKO, Carpinteria, CA) diluted 1:100 overnight at 4°C.

PCNA IF. PCNA staining is used to assess proliferation mostly in TA zone (or above +4). Non-specific antibody binding was blocked 20% goat serum for 30 minutes at RT. Sections

were incubated overnight at 4 °C in a humidified chamber with 1:100 diluted mouse-anti-PCNA (sc-56; Santa Cruz Biotechnology, Santa Cruz, CA). Then the sections were incubated with AlexaFluor-594 goat anti-mouse secondary antibodies (1:100; A11001, Invitrogen) for 1 hour at room temperature and counterstained with VectaShield plus DAPI (Vector Laboratories).

3.2 Intestinal differentiation markers

Pan-Cytokeratin. Pan-cytokeratin identifies intestinal epithelial cells (Leibowitz et al., 2011). Non-specific antibody binding was blocked using 15% goat serum for 30 minutes at room temperature, incubated overnight at 4°C with mouse-anti-pan-cytokeratin (ab961; AE1 + AE3; prediluted; Abcam, Cambridge, MA). Sections were then and counterstained with VectaShield + DAPI (Vector Laboratories).

Figure 6. Donor BM-derived cells (green) in the intestinal of the recipient mouse outlined by cytokeratin staining (Leibowitz et al., 2014b).

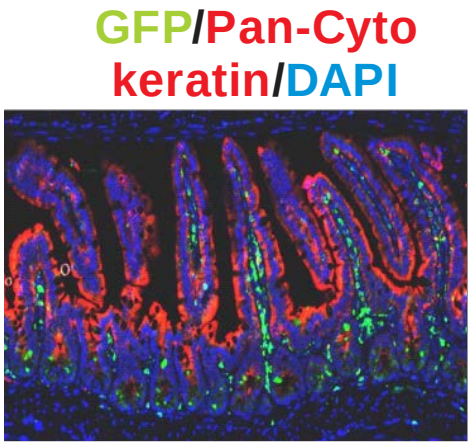

MMP-7 and Cryptdin 4 IHC. MMP-7 and cryptidin 4 identify Paneth cells, which are part of the Lgr5+ cell niche and anchored at the crypt bottom in healthy mice (Sato et al., 2011). Non-specific antibody binding was blocked using the 20% goat or rabbit serum for 30 min. The sections were incubated with a goat-anti-MMP-7 (Wilson et al., 1999) (eBioscience, San Diego, CA) or a rabbit cryptdin 4 antiserum (Ouellette et al., 1999) (from Michael Selsted, University of California, Irvine, CA), at 1:50 dilution at RT for 2 hour or at 4°C overnight. The signals were detected with the ABC kit and DAB kit (Vector laboratory). The sections were counter-stained with hematoxylin.

Figure 7. Paneth cells are marked by MMP-7 and Cryptdin 4 IHC (Qiu et al., 2008).

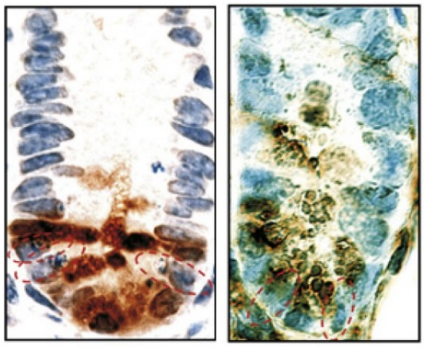

Lysozyme IF is also commonly used for detecting Paneth cells (Qiu et al., 2009b). Non-specific antibody binding was blocked using 20% goat serum for 30 min. The sections were incubated with goat polyclonal anti-lysozyme (sc-27958, Santa Cruz, Santa Cruz, CA) at 1:50 dilution at 4°C overnight. Antibody-antigen complexes were visualized by incubation with Alexa Fluor 594 (Invitrogen, Carlsbad, CA), and counterstained with DAPI (Vector Laboratories, Burlingame, CA).

Mucin 2 (Muc2) IF. Muc 2 marks Goblet cells. Non-specific antibody binding was blocked using 20% rabbit serum for 30 min at RT. Sections were incubated with rabbit polyclonal anti-Mucin2 antibody (cat#sc15334, Santa Cruz, Santa Cruz, CA) at 1:100 dilution at 4°C overnight. Antibody-antigen complexes were visualized by incubation with Alexa Fluor 594 (Invitrogen,

Carlsbad, CA). Sections were then counterstained with VectaShield + DAPI (Vector Laboratories). Cells with positive staining were scored in at least 100 crypts or villi and reported as mean ± SD. Three or more mice were used in each group.

Chromogranin A IF. Chromogrannin A identifies enteroendocrine cells. Non-specific antibody binding was blocked using 20% goat serum for 30 min at RT. Sections were incubated with rabbit polyclonal anti-ChA (cat# ab15160, Abcam, Cambridge, MA) at 1:50 dilution at 4℃ overnight. Antibody-antigen complexes were visualized by incubation with Alexa Fluor 594 (Invitrogen, Carlsbad, CA). Sections were then counterstained with VectaShield + DAPI (Vector Laboratories). Cells with positive staining were scored in at least 100 crypts or villi and reported as mean ± SD.

Figure 8. Intestinal differentiation detected by IF (Wang X unpublished and (Qiu et al., 2013)).

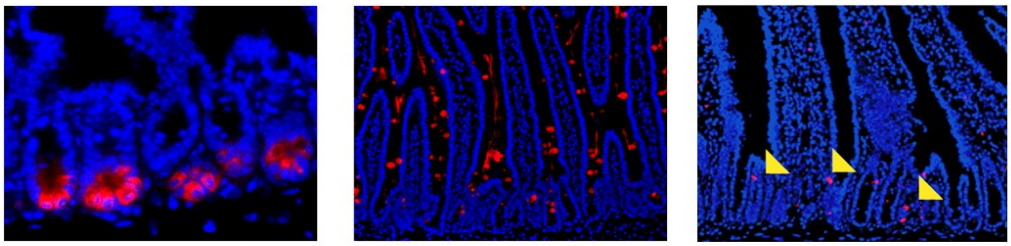

3.3 DNA damage and repair

γH2AX IF. **γH2AX** identifies DNA double-strand breaks. Non-specific antibody binding was blocked using 20% goat serum at room temperature for 1 hour. Sections were incubated overnight at 4°C in a humidified chamber with 1:100 diluted Mouse-anti- γH2AX (#05-636; Millipore, Billerica, MA). The sections were incubated with AlexaFluor-594 goat-anti-mouse secondary antibodies (1:100; A11005, Invitrogen) for 1 hour at room temperature and counterstained with VectaShield plus DAPI (Vector Laboratories).

pRPA32 IF. pRPA identifies replication stress and stalled replication forks. Non-specific antibody binding is blocked using 20% goat serum for 30minutes at room temperature, and incubated overnight at 4°C with 1:100 diluted rabbit anti-phospho-RPA32 (T21; ab61065; Abcam, Cambridge, MA). Sections were then incubated for 1 hour at room temperature with AlexaFluor 488-conjugated goat-anti-rabbit secondary antibodies (1:200; Invitrogen) and counterstained with VectaShield + DAPI (Vector Laboratories).

Figure 9. DNA damage detection in the crypts (Wang X unpublished (Wang et al., 2016))

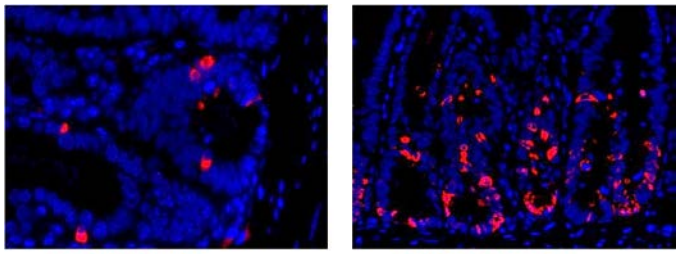

53BP1 IF. 53BP1 is a key DNA damage and repair protein, and persistent foci can indicate unrepaired damage. Non-specific antibody binding was blocked using 20% goat serum at room temperature for 1 hour. Sections were incubated overnight at 4°C in a humidified chamber with 1:100 diluted Mouse-anti- 53BP1 (IHC-00001; Bethyl Laboratories). Then the sections were incubated with AlexaFluor-594 goat-anti-mouse secondary antibodies (1:100; A11005, Invitrogen) for 1 hour at room temperature and counterstained with VectaShield plus DAPI (Vector Laboratories).

BRCA1 IF. BRCA1 is a key DNA repair protein involved in homologous recombination-mediated (HR) repair. Non-specific antibody binding was blocked using 20% goat serum at room temperature for 1 hour. Sections were incubated overnight at 4°C in a humidified chamber with 1:100 diluted Rabbit-anti- BRCA1 (S1387) (NB100-225; Novus, Littleton CO, USA). Then the sections were incubated with AlexaFluor-594 goat-anti-Rabbit secondary antibodies (1:100; A11005, Invitrogen) for 1 hour at room temperature and counterstained with VectaShield plus DAPI (Vector Laboratories).

RAD51 IF. RAD51 is a key DNA repair protein involved in homologous recombination-mediated (HR) repair. Non-specific antibody binding were blocked using 20% goat serum at room temperature for 1 hour. Sections were incubated overnight at 4°C in a humidified chamber with 1:100 diluted Mouse-anti- RAD51 (ab1837; Abcam, Cambridge, MA, USA). Then the sections were incubated with AlexaFluor-594 goat-anti-mouse secondary antibodies (1:100; A11005, Invitrogen) for 1 hour at room temperature and counterstained with VectaShield plus DAPI (Vector Laboratories).

DNA-PKcs IF. DNA-PKcs is a key DNA repair protein involved in non-homologous end joining (NHEJ). Non-specific antibody binding was blocked using 20% goat serum at room temperature for 1 hour. Sections were incubated overnight at 4°C in a humidified chamber with 1:100 diluted Mouse-anti- DNA-PKcs (#ab18356; Abcam, Cambridge, MA, USA). Then the sections were incubated with AlexaFluor-594 goat-anti-mouse secondary antibodies (1:100; A11005, Invitrogen) for 1 hour at room temperature and counterstained with VectaShield plus DAPI (Vector Laboratories).

Figure 10. Repair proteins rapidly form foci at damage sites to direct DNA repair via different pathways. Indicated foci in the crypts 4 hr after 15 Gy TBI are visualized by confocal microscopy and quantitated (Wei et al., 2016).

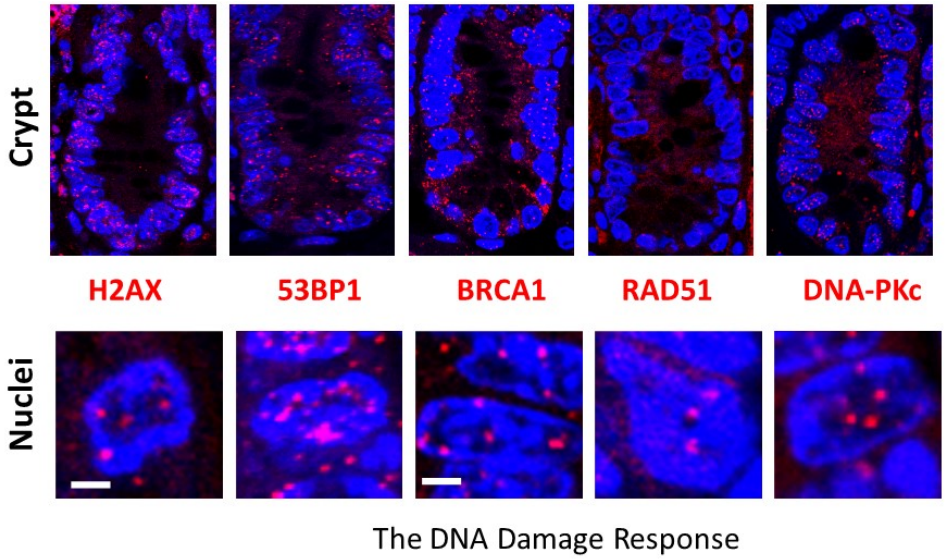

The DNA Damage Response

3.4 Barrier, immune and BM-derived cells

Loss of epithelial cells or inadequate or abnormal epithelial regeneration leads to barrier defects, which can be structural with obvious loss of crypts and shortening of villi, or functional due to the loss or reduction of tight junctions between epithelial cells. Intestinal barrier and permeability can be altered without obvious structural changes such as crypt number and crypt size, or villus shape or height. We and others showed that TBI causes rapid and persistent decrease of tight junction proteins. Breaching the intestinal epithelial barrier leads to increased contact of immune cells with luminal antigens and bacteria which triggers inflammation, correlated with infiltration of various BM-derived (CD45+) cells including various immune cells. Radiation also damages BM-derived cells (CD45+), including endothelial (CD31+ or CD105+) cells more prominently located in the villi (Leibowitz et al., 2014b; Qiu et al., 2008), and believe to regulate intestinal injury and regeneration. Here, we selected some representative populations detected by staining in the small intestine. Flow cytometry can conceivably be used to more precisely enrich and quantitate immune subpopulations going forward, though challenging with the extent of tissue injury after high dose TBI, therefore not covered here.

3.4.1 Tight junction proteins

The increase of permeability can be caused by drastic changes in the components of tight junctions such as zonula occludens (ZO1 and ZO2), Occludin (reduced), Claudin-1(induced), which can be detected by staining or RT-PCR.

ZO-1 IF. ZO-1 identifies tight junctions between intestinal epithelial cells. Non-specific antibody binding was blocked using 20% rabbit serum for 30 min at RT. Sections were incubated with rabbit polyclonal anti-ZO-1 (cat# 61-7300, Thermo Fisher Scientific, Fremont, CA) at 1:100 dilution at 4℃ overnight. Antibody-antigen complexes were visualized by incubation with Alexa Fluor 594 (Invitrogen, Carlsbad, CA). Sections were then counterstained with VectaShield + DAPI (Vector Laboratories).

Figure 11. Tight junction proteins detected by IF in the intestinal epithelium (Wei L *et. al.* unpublished).

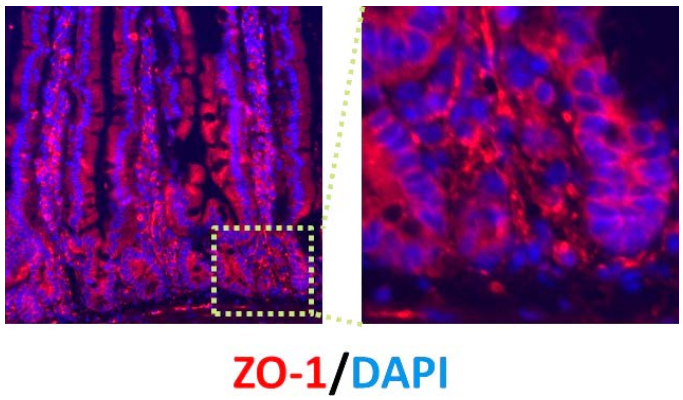

3.4.2 Immune cells.

In the healthy intestine, there is minimal presence of immune cells such as T cells, B cells, macrophages or neutrophils, which can be recruited after TBI or other types of injury (i.e. inflammation).

Immune marker IF. Non-specific antibody binding was blocked using 20% rabbit serum for 30 min. Sections were stained with rat monoclonal anti-Neutrophil antibody (#MCA771GT, AbD serotec, Raleigh, NC) at 1:100 dilution, rabbit anti-Cd45R (B220) (B cell marker) (clone AR3-6B2, #25-0452, eBioscience, San Diego, CA) at 1:50 dilution, rabbit anti-CD3epsilon (T cell marker) (#RB-360-A0, Thermo Fisher Scientific, Fremont, CA) at 1:50 dilution, or rabbit anti-Ly-6G (Gr-1) (myeloid marker) (clone RB6-8C5) (#550291, BD Biosciences, San Jose, CA) at 1:50 dilution at 4℃ overnight, respectively. Antibody-antigen complexes were visualized by incubation with Alexa Fluor 594 (Invitrogen, Carlsbad, CA), and counterstained with DAPI (Vector Laboratories, Burlingame, CA). Cells with positive staining were scored in at least 100 crypts or villa and reported as mean ± SD. Three or more mice were used in each group.

Figure 12. Prominent immune cell infiltration following ISC loss in *ADAR1* KO small intestine (Qiu et al., 2013).

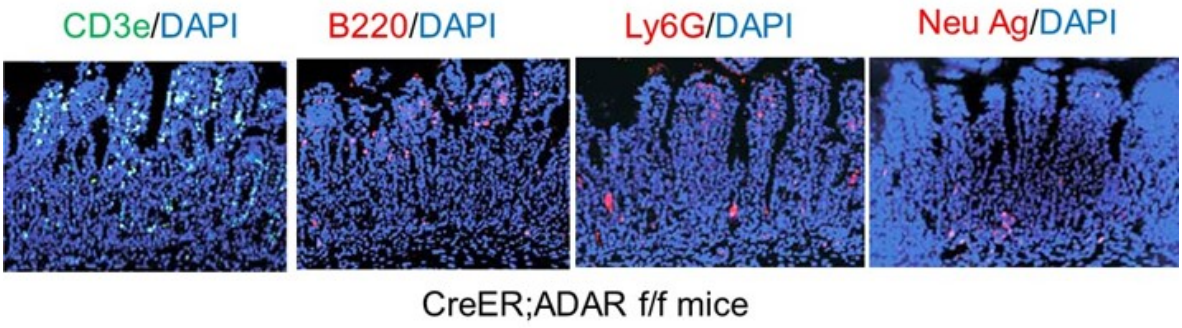

3.4.3 BM-derived cells and endothelial cells in the villi

CD45 IF. Slides were incubated with Rat anti-mouse CD45 antibodies (1:50; 553076; BD Biosciences) at 4℃ overnight, then incubated with AlexaFluor-594 goat-anti-Rat secondary antibodies (1:100; A11007; Invitrogen) for 1 hour at room temperature. Sections were counterstained with VectaShield plus DAPI (Vector Labs).

CD105 IF. Slides were incubated with Rat anti-mouse CD105 antibodies (1:50; 14-1051-82; eBioscience, San Diego, CA) at 4℃ overnight, then incubated with AlexaFluor-594 goat-anti-Rat secondary antibodies (1:100; A11007; Invitrogen) for 1 hour at room temperature. Sections were counterstained with VectaShield plus DAPI (Vector Labs).

Figure 13. Loss of CD45+ and CD105+ cells in the villi after 15 Gy TBI (Leibowitz et al., 2014b).

Section 4. Intestinal Stem Cell Analysis

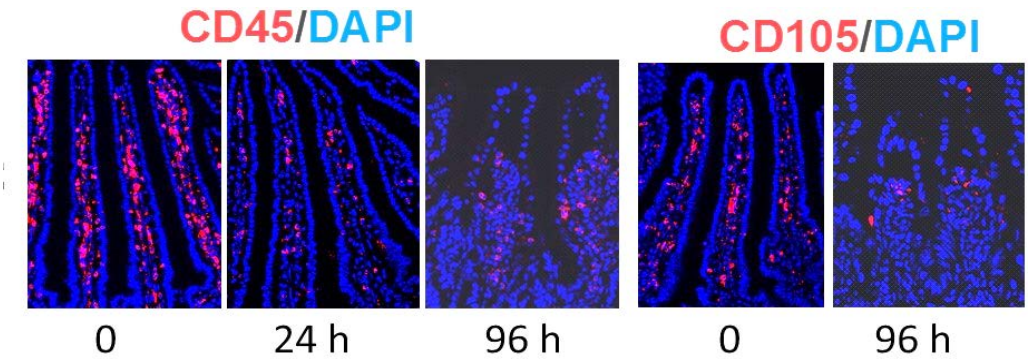

High doses of radiation cause loss of CBCs (Hua et al., 2012; Qiu et al., 2008; Yan et al., 2012), and activation of quiescent stem cells (Barker et al., 2012; Yan et al., 2012), which appears heterogeneous at the level of markers, including label retaining cells (LRC) (Buczacki et al., 2013), delta ligand expressing Dll1+ cells (van Es et al., 2012), and Sox9-GFP high cells (Van Landeghem et al., 2012), many also express Lgr5 in the +4 region (+3-+7) adjacent and mixed with transiently amplifying (TA) cells. Several methods can be used to enrich stem cells, while in-depth gene expression analysis (Munoz et al., 2012) and single cell transcript analysis (Itzkovitz et al., 2012) are still lacking to understand the true signature of "radio-resistant" intestinal stem cells and how they are activated by regeneration. The most robust method so far has been the use of Lgr5-EGFP-IRES-creERT2 mice (Barker et al., 2007) to study Lgr5 cells. Several groups have used a combination of cell surface markers for ISC enrichment and isolation in both mouse and human (Gracz et al., 2013; Magness et al., 2013; Wang et al., 2013), which is not covered here. Stem cells are defined by function and closely related to early progenitors in gene expression and even potentially "stemness" induced by injury. Therefore, short- and long-term assays should be considered to evaluate stem cell injury and recovery at different levels, such as their numbers, interaction with their niche, potentials in self-renewal and differentiation and to maintain the barrier.

4.1 Stem cell number, location and self-renewal

GFP/Lgr5 IF. *Lgr5-EGFP (Lgr5-EGFP-IRES-creERT2)* mice (Barker et al., 2007) are the most widely used for isolation and characterization ISC based on Lgr5-driven GFP expression (Barker et al., 2012). Non-specific antibody binding was blocked using 20% goat serum at room temperature for 1 hour. Sections were incubated overnight at 4 °C in a humidified chamber with 1:100 diluted mouse-anti-GFP (sc-9996; Santa Cruz Biotechnology, Santa Cruz, CA). Then the sections were incubated with AlexaFluor-488 goat anti-mouse secondary antibodies (1:100; A11001, Invitrogen) for 1 hour at room temperature and counterstained with VectaShield plus DAPI (Vector Laboratories). Co-stain of Lgr5 with TUNEL and other markers allows ISC specific assessment (Qiu et al., 2010; Wang et al., 2015).

Lgr5 lineage tracing. The activity of Lgr5 cells is assessed using a β-Galactosidase reporter following induction of Lgr5 driven CRE and tissue whole mount staining (Barker et al., 2007). 10 mg/ml tamoxifen (T5648; Sigma; 100 mg/kg) in corn oil (Cat# C8267 , Sigma) is given through intraperitoneal injection 18 hours prior to IR in *Lgr5-EGFP/Rosa*$^{B/+}$ (LacZ reporter) mice. The top 1/3 of the small intestine (~10 cm) was collected and fixed at 4°C (1% Formaldehyde, 0.2% Glutaraldehyde and 0.02% NP-40 in PBS) 96 hours after IR. After twice washing, the small intestines were stained overnight at room temperature in the dark on rolling platform (5 mM $K_3Fe(CN)_6$, 5 mM $K_4Fe(CN)_6 \cdot 3H_2O$, 2 mM $MgCl_2 \cdot 6H_2O$, 1 mg/ml X-Gal, 0.02% NP40 and 0.1% NaDeo in PBS). Whole-mount tissues were fixed in 4% paraformaldehyde and photographed, then Swiss-rolled and followed by paraffin embedding. The whole-mount pictures were taken with an Olympus SZX10 stereo microscope equipped with a DP26, 5MP high-fidelity digital color camera and CellSens imaging software. Embedded tissues were cut into 5 µm sections and stained by Eosin as described in H&E staining and photographed. The numbers and fractions of entirely blue crypts were quantitated in 3 longitudinal 10-cm jujenal sections (Wei et al., 2016).

Figure 14. A CDK4/6 inhibitor (PD) blocks TBI-induced Lgr5+ cell apoptosis and improves Lgr5 lineage tracing (Wei et al., 2016).

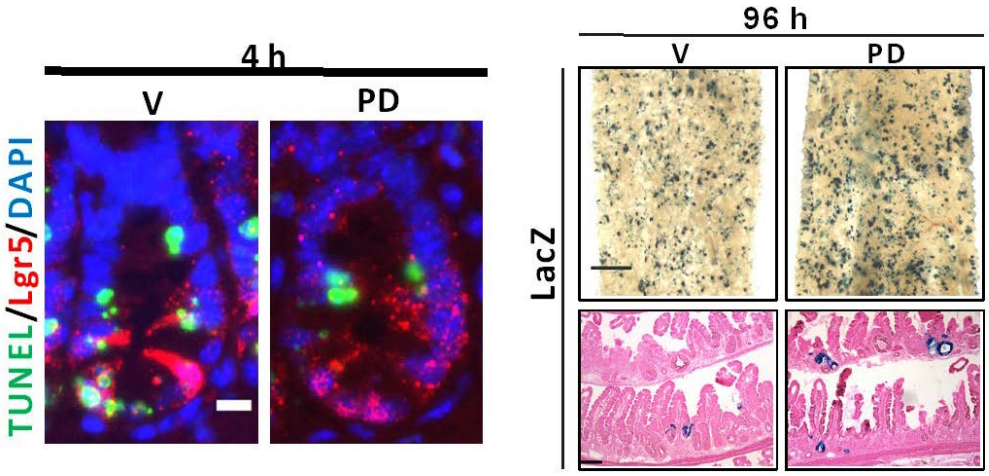

OLFM4 RNAscope In Situ Hybridization (ISH) Assay. *OLFM4* and *Lgr5* are widely used ISC markers that can be reliably detected by RNA ISH or RNAscope (Qiu et al., 2009a; Qiu et al., 2013; Wei et al., 2016), while detection of respective proteins by antibodies in mouse crypts remains challenging. *Lgr5* detection is more difficult due to much lower expression levels than

OLFM4. Murine *OLFM4* probe (Cat# 311831 and RNAscope® 2.0 HD Reagent Kit-Brown#310035) were purchased from Advanced Cell Diagnostics (ACD, Hayward, CA) and used according to the manufacturer's instructions. Deparaffinized 5-μm paraffin sections were pre-treated with Pretreat 1, 2 and 3. *Olfm4* was added to the slides and incubated in the HybEZ oven (310010; ACD) for 2 hours at 40°C. After 6 signal amplification steps, tissue expression was detected by DAB and counterstained. Slides were mounted with Crystal Mount (#M02, Biomeda, Texarkana, AR) and photographed.

Figure 15. ISCs identified using *OLFM4* RNAscope, *OLFM4* and *Lgr5* RNA ISH (Qiu et al., 2009a; Qiu et al., 2013; Wei et al., 2016).

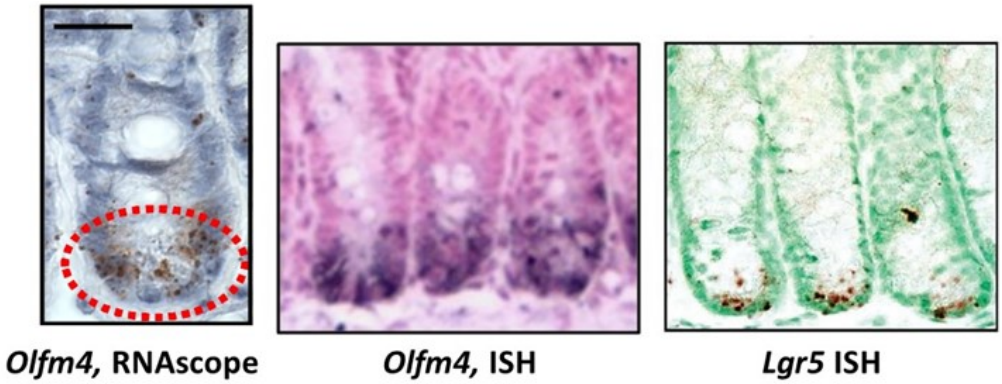

4.2 Stem Cell Isolation

Isolation of Lgr5+ cells from mouse intestine

Lgr5/GFP positive stem cells were isolated from Lgr5-EGFP-IRES-creERT2 mice as described (Barker et al., 2007; Sato et al., 2009), with minor modifications (Qiu et al., 2013). The proximal intestine segment (jejunum, ~10-cm) were collected, flushed gently with cold phosphate-buffered saline (PBS), and opened longitudinally in a tissue culture dish. Following one PBS rinse, tissues were incubated in PBS containing 30 mM ethylenediaminetertaacetic acid (EDTA) and 1.5 mM DL-Dithiothreitol (Sigma-Aldrich, St. Louis, MO) on ice for 20 min. Intestinal tissues were transferred to a 15 ml conical tube containing 5 ml of 30 mM EDTA in PBS, incubated at 37°C for 8 min, then shaken by hand for 30 seconds at 3 shake cycles per second. After shaking, the remnant muscle layer was discarded, and the dissociated cells were pelleted at 800g, resuspended in PBS + 10% fetal bovine serum (FBS) and repelleted at 400g. The cells were then incubated in 10 ml of modified Hank's buffered salt solution (mHBSS) containing 0.3 U/ml of dispase (BD Biosciences, Bedford MA) at 37°C for 10 min with intermittent shaking every 2 mins for 30 sec to dissociate epithelial sheets to single cells. 1 ml FBS and 1000 U DNase (AppliChem, St. Louis, MA) was added to cell suspension and then was sequentially passed through 70 μM and 40 μM filters (BD Biosciences, Bedford, MA). Cells were pelleted and resuspended in 10 ml HBSS and then repelleted and resuspended at a concentration of 2×10^7 cells/ml in intestinal epithelial stem cell (IESC) media (Advanced DMEM/F12 supplemented with 1× N2, 1× B27, 10 mM HEPES, 10 μM Y27632, 100 ug/ml Penicillin/Streptomycin). Approximately 1×10^7 cells were incubated in 1 ml IESC media with antibodies [α-CD31-PE/Cy7 (Biolegend), α-CD45-PE/Cy7 (Biolegend), and DAPI on ice for 30

min with mixing every 10 min. The CD31 /CD45/DAPI tripled negative population are sorted as total intestinal epithelial cells, and Lgr5 high and low fractions, 10,000-30,000 cells each can be used for further analysis. Two or more mice were used.

Figure 16. Lgr5+ cells sorted from mice (Qiu et al., 2013). Isolation and characterization of Lgr5 cells from irradiated mice is more difficult but ongoing.

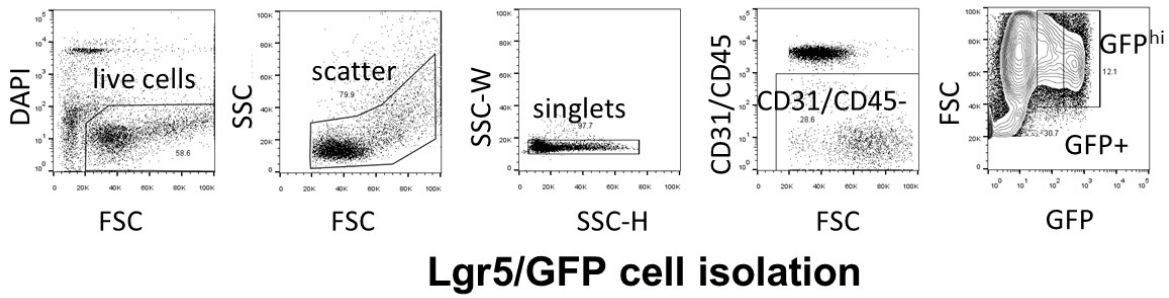

4.3 Intestinal crypt and stem cell culture

4.3.1 Primary culture of intestinal stem cell or crypt culture

Isolated ISCs can grow *in vitro* into budding structures that contain both stem cells and differentiated populations with the matrix and a cocktail of growth factors (Sato et al., 2009). These structures contain only epithelial cells and therefore termed enteroids (Stelzner et al., 2012), opposed to organoids containing multiple cell types. This *"in vitro"* clonogenic assay can be used to assess stem cell renewal, proliferation, and differentiation in radiation studies. Crypt culture is subjected to less manipulation and more commonly used (Qiu et al., 2013; Wang et al., 2015).

Mouse crypts are isolated and cultured as published (Qiu et al., 2013; Sato et al., 2009). A total of 500 crypts were mixed with 50 μl Matrigel (Cat# 356231, BD Bioscience, Bedford, MA) and plated in 24-well plates. After gelling of Matrigel, 500 μl of crypt culture medium [Advanced DMEM/F12 (Cat# 12634-010, Invitrogen, Grand Island, NY) containing 50 ng/ml EGF (Cat# 315-09, Peprotech, Rocky Hill, NJ), 100 ng/ml Noggin (Cat# 250-38, Peprotech, Rocky Hill, NJ), 500 ng/ml R-spondin 1 (Cat#4645-RS, R&D Systems, Minneapolis, MN), 1 mM N-Acetylcysteine (Cat# A9165, Sigma-Aldrich, St. Louis, MO), 1% N2 supplement (Cat# 17502-048, Invitrogen, Grand Island, NY) and B27 supplement (Cat# 12587-010, Invitrogen, Grand Island, NY)] is added.

4.3.2 Passage of crypt culture

Crypt cultures can be established using mice of different genotypes, and passaged several times in culture. Using passages reduces the usage on mice and provides more consistent results as cultures can be grown and split at the same time prior to desired treatments to avoid mouse and isolation-associated variability. For passage, enteroids are removed from Matrigel and mechanically dissociated into single crypt domains and then transferred to fresh Matrigel. Passage is performed every 5 days with a 1:3 split ratio. This can be repeated several times up to a month in culture (Wang et al., 2015), and used to screen for radiation protectors or mitigators

(Wang et al., 2015). Known radiation protectors of mitigators can be added at desirable times to assess their effects on enteroid growth and responses.

Figure 16. Mouse crypt culture with Lgr5+ cells and differentiated cells (Wang et al., 2015).

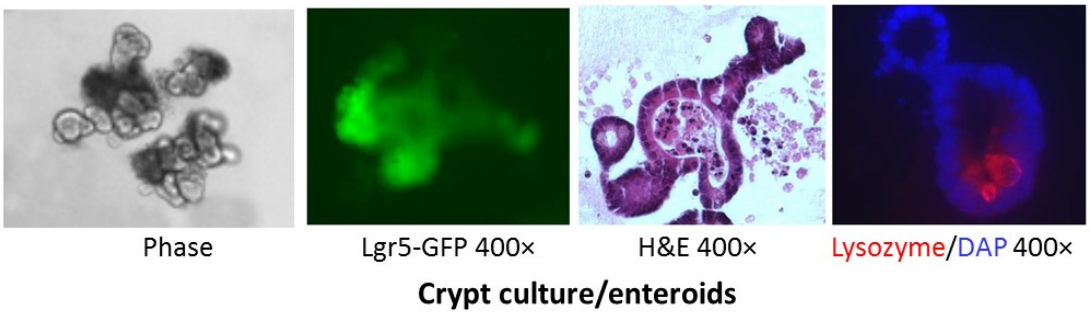

4.3.3 Radiation of crypt culture

Crypt cultures, usually after 1-2 passages with robust growth, were irradiated at 5 Gy, or several doses, 24h after plating. Enteroid growth was quantified 5 days after radiation in primary culture and 4 days after radiation in passaged cultures, and shows a clear dose-response (20). Using the growth-based assay coupled with molecular analyses, one can assess the effects of genotype, growth factor , small molecule, or adenoviral gene transduction (Wang et al., 2015), as well as conditional gene ablation (Qiu et al., 2013). Human crypt cultures using slightly different factors and growth medium were used to confirm the critical role of p53-mediated apoptosis and PUMA induction in radiation-induced intestinal toxicity (Wang et al., 2015). These assays complement mouse models to help established epithelial intrinsic mechanisms, as well as help identify novel intestinal radiation protectors and mitigators as we and others have done.

Figure 16. Growth, apoptosis, DNA damage, and ISC maker expression in irradiated crypt culture (Wang et al., 2015).

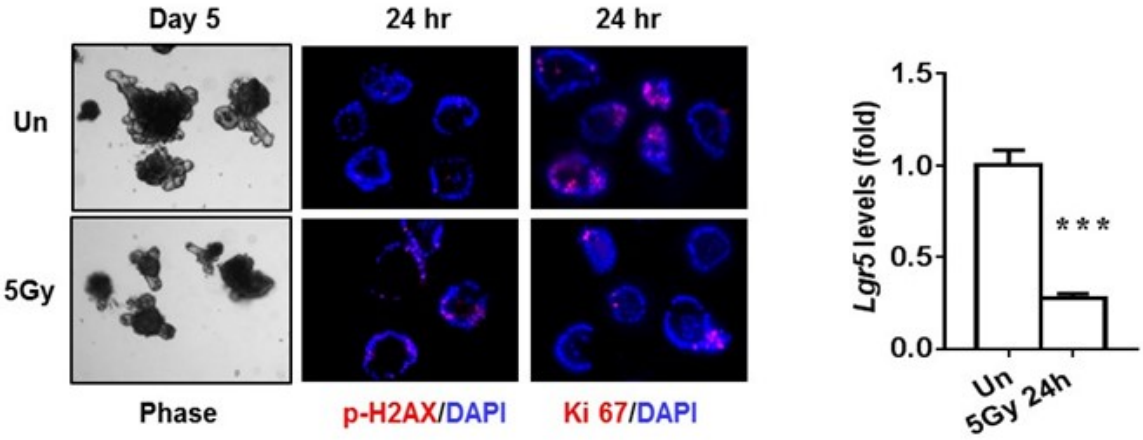

4.3.4 Staining and molecular analysis of crypt culture

Crypt cultures were harvested at desired times i.e., 4 h or 24 h after radiation (5 Gy or desired doses), fixed with 10% formalin and mixed with 2% agarose and then processed (Qiu et al., 2013; Wang et al., 2015). Sections (5 μm) from paraffin-embedded crypt enteroids were subjected to immunostaining for apoptosis, proliferation, DNA damage response, or stem cells using similar methods as intestinal sections described before. Protein and RNA were isolated form crypt culture following digestion of the Matrigel with Cell Recovery Solution (Cat# 354253, BD Bioscience, Bedford, MA) for molecular analysis (Qiu et al., 2013; Wang et al., 2015) is described below.

5. Molecular analyses on protein and mRNA

These analyses are highly question- and pathway-specific, selection of markers and methods should be driven by the scientific question. Due to limited material of isolated intestinal stem cells, analyses are mostly mRNA-based, using either (or both) RT-PCR for validation, or transcriptome analysis for discovery purposes. Protein confirmation is generally done by *in situ*/staining or co-staining to identify cell position and origin.

5.1 Western blotting

Total protein was prepared from freshly isolated small intestine by optimizing several protocols (Leibowitz et al., 2014a; Qiu et al., 2008; Wu et al., 2007). Immediately after sacrifice, the entire small intestines were carefully isolated and placed on ice. The duodenum was removed, and the rest of the intestine (~30 cm) was divided into two equal segments, representing the proximal (jejunum) and distal (ileum) segments. The segments were rinsed thoroughly with ice cold physiological saline. The jejunal or ileum segments of 3-6 mice from each group were opened longitudinally on the antimesenteric border to expose the intestinal mucosa. The mucosal layers were harvested by gentle scraping with a glass slide. The scraping samples were stored at -80°C before the analysis.

The scraping was put into 600 uL homogenization buffer (0.25 M sucrose, 10 mM Hepes, and 1 mM EGTA) supplemented with protease inhibitors (Complete mini, EDTA-free; Roche) and homogenized with 25 strokes in a Dounce homogenizer by using a “loose” pestle, followed by 25 strokes with a “tight” pestle. Samples were then cleared by two rounds of centrifugation at 1,000 × g for 10 min at 4 °C. Cleared lysate was assayed for protein concentration and stored at −80 °C. The “cleared lysate” provides clearer blots with certain antibodies compared to direct lysis of the scraping by protein sample buffer. To further increase signals, cytoplasmic or nuclear fractions can be prepared using NE-PER® Nuclear and Cytoplasmic Extraction Reagents (Cat#78833, ThermoFisher) or other compatible methods. Extract was mixed with protein sample buffer and analyzed by NuPage gel (Invitrogen, Carlsbad, CA) electrophoresis. We have successfully analyzed a number of DDR-related markers such as the p53 pathway and DNA repair-associated proteins.

5.2. RT-PCR

Total cellular RNA was isolated from approximately 100 mg of minced fresh tissues (intestinal epithelium scraping), cultured crypts pulled from 3 wells from 24-well plates, or 10,000 to 30,000 Lgr5+ or ISC marker enriched populations by flow cytometry using the Mini-RNA Isolation II Kit (Cat# R1055, Zymo Research) according to the manufacturer’s protocol.

Complementary DNA was generated using SuperScript III reverse transcriptase (Invitrogen) with random priming. Real-time PCR was performed on CFX96 (Bio-Rad, Hercules, CA) with SYBR Green (Invitrogen, Carlsbad, CA). We have routinely analyzed many different gene sets related to stress response, p53 pathway, NF-κB targets/inflammatory cytokines, Wnt targets, ISC markers, differentiation makers, and tight junction markers among others (Qiu et al., 2008; Qiu et al., 2013; Qiu et al., 2010; Qiu et al., 2011). Melting curve and agarose gel electrophoresis of the PCR products were used to verify the specificity of PCR amplification. Transcriptome analysis using cDNA microarray of RNA sequencing employs a variety of specific algorithms or programs for gene and differential expression call and further analyses on data and pathways, and therefore covered here.

Figure 17. Radioprotection of crypt culture by a GSK inhibitor (GSKi). GSKi radio-protects crypts in culture by blocking p53K120-dependent PUMA but not p21 induction (A-B). The survival advantage was lost upon Ad-PUMA expression (C-D) (Wang et al., 2015).

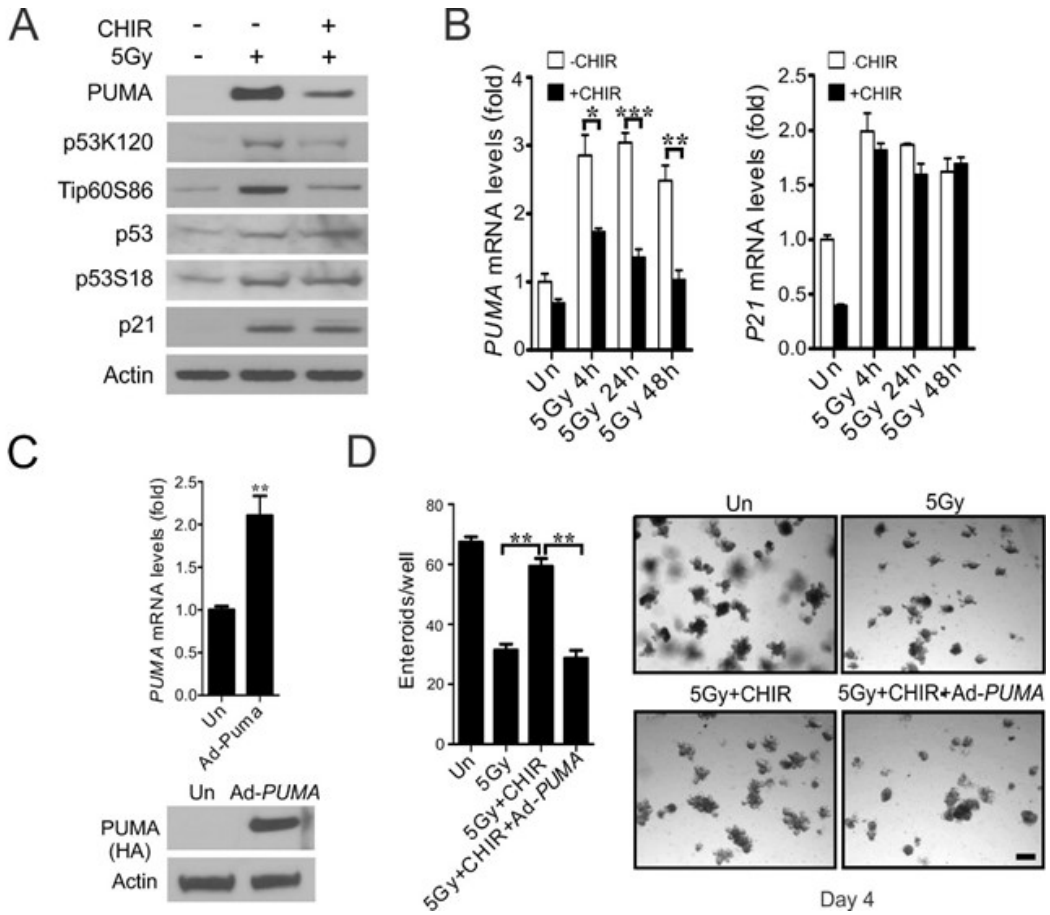

Section 6. Statistical analysis

Statistical analyses were performed using GraphPad Prism software (La Jolla, CA 92037 USA). Survival was analyzed by the Log-rank test. Data from staining were analyzed by unpaired Student's t-test (two-tailed) or analysis of variance (ANOVA) followed by Turkey's or

Bonferroni's Test in which multiple comparisons were performed using the method of least significant difference. *P* values were considered significant if $p < 0.05$.

References

Barker, N., van Es, J.H., Jaks, V., Kasper, M., Snippert, H., Toftgard, R., and Clevers, H. (2008). Very Long-term Self-renewal of Small Intestine, Colon, and Hair Follicles from Cycling Lgr5+ve Stem Cells. Cold Spring Harb Symp Quant Biol.

Barker, N., van Es, J.H., Kuipers, J., Kujala, P., van den Born, M., Cozijnsen, M., Haegebarth, A., Korving, J., Begthel, H., Peters, P.J., *et al.* (2007). Identification of stem cells in small intestine and colon by marker gene Lgr5. Nature *449*, 1003-1007.

Barker, N., van Oudenaarden, A., and Clevers, H. (2012). Identifying the stem cell of the intestinal crypt: strategies and pitfalls. Cell Stem Cell *11*, 452-460.

Berbee, M., and Hauer-Jensen, M. (2012). Novel drugs to ameliorate gastrointestinal normal tissue radiation toxicity in clinical practice: what is emerging from the laboratory? Curr Opin Support Palliat Care *6*, 54-59.

Bjerknes, M., and Cheng, H. (1999). Clonal analysis of mouse intestinal epithelial progenitors. Gastroenterology *116*, 7-14.

Bjerknes, M., and Cheng, H. (2005). Gastrointestinal stem cells. II. Intestinal stem cells. Am J Physiol Gastrointest Liver Physiol *289*, G381-387.

Buczacki, S.J., Zecchini, H.I., Nicholson, A.M., Russell, R., Vermeulen, L., Kemp, R., and Winton, D.J. (2013). Intestinal label-retaining cells are secretory precursors expressing Lgr5. Nature *495*, 65-69.

Dekaney, C.M., Rodriguez, J.M., Graul, M.C., and Henning, S.J. (2005). Isolation and characterization of a putative intestinal stem cell fraction from mouse jejunum. Gastroenterology *129*, 1567-1580.

Gracz, A.D., Fuller, M.K., Wang, F., Li, L., Stelzner, M., Dunn, J.C., Martin, M.G., and Magness, S.T. (2013). CD24 and CD44 Mark Human Intestinal Epithelial Cell Populations with Characteristics of Active and Facultative Stem Cells. Stem Cells.

Greenberger, J.S. (2009). Radioprotection. In Vivo *23*, 323-336.

Harper, J.W., and Elledge, S.J. (2007). The DNA damage response: ten years after. Mol Cell *28*, 739-745.

Hauer-Jensen, M., Denham, J.W., and Andreyev, H.J. (2014). Radiation enteropathy--pathogenesis, treatment and prevention. Nat Rev Gastroenterol Hepatol *11*, 470-479.

Hua, G., Thin, T.H., Feldman, R., Haimovitz-Friedman, A., Clevers, H., Fuks, Z., and Kolesnick, R. (2012). Crypt base columnar stem cells in small intestines of mice are radioresistant. Gastroenterology *143*, 1266-1276.

Itzkovitz, S., Lyubimova, A., Blat, I.C., Maynard, M., van Es, J., Lees, J., Jacks, T., Clevers, H., and van Oudenaarden, A. (2012). Single-molecule transcript counting of stem-cell markers in the mouse intestine. Nat Cell Biol *14*, 106-114.

Kirsch, D.G., Santiago, P.M., di Tomaso, E., Sullivan, J.M., Hou, W.S., Dayton, T., Jeffords, L.B., Sodha, P., Mercer, K.L., Cohen, R., *et al.* (2010). p53 Controls Radiation-Induced Gastrointestinal Syndrome in Mice Independent of Apoptosis. Science *327*, 593-596.

Leibowitz, B., Qiu, W., Buchanan, M.E., Zou, F., Vernon, P., Moyer, M.P., Yin, X.M., Schoen, R.E., Yu, J., and Zhang, L. (2014a). BID mediates selective killing of APC-deficient cells in intestinal tumor suppression by nonsteroidal antiinflammatory drugs. Proc Natl Acad Sci U S A *111*, 16520-16525.

Leibowitz, B.J., Qiu, W., Liu, H., Cheng, T., Zhang, L., and Yu, J. (2011). Uncoupling p53 Functions in Radiation-Induced Intestinal Damage via PUMA and p21. Mol Cancer Res *9*, 616-625.

Leibowitz, B.J., Wei, L., Zhang, L., Ping, X., Epperly, M., Greenberger, J., Cheng, T., and Yu, J. (2014b). Ionizing irradiation induces acute haematopoietic syndrome and gastrointestinal syndrome independently in mice. Nat Commun *5*, 3494.

Magness, S.T., Puthoff, B.J., Crissey, M.A., Dunn, J., Henning, S.J., Houchen, C., Kaddis, J.S., Kuo, C.J., Li, L., Lynch, J., *et al.* (2013). A multicenter study to standardize reporting and analyses of fluorescence-activated cell-sorted murine intestinal epithelial cells. Am J Physiol Gastrointest Liver Physiol *305*, G542-551.

Mandal, P.K., Blanpain, C., and Rossi, D.J. (2011). DNA damage response in adult stem cells: pathways and consequences. Nat Rev Mol Cell Biol *12*, 198-202.

Marshman, E., Booth, C., and Potten, C.S. (2002). The intestinal epithelial stem cell. Bioessays *24*, 91-98.

Metcalfe, C., Kljavin, N.M., Ybarra, R., and de Sauvage, F.J. (2014). Lgr5+ stem cells are indispensable for radiation-induced intestinal regeneration. Cell Stem Cell *14*, 149-159.

Montgomery, R.K., Carlone, D.L., Richmond, C.A., Farilla, L., Kranendonk, M.E., Henderson, D.E., Baffour-Awuah, N.Y., Ambruzs, D.M., Fogli, L.K., Algra, S., *et al.* (2011). Mouse telomerase reverse transcriptase (mTert) expression marks slowly cycling intestinal stem cells. Proc Natl Acad Sci U S A *108*, 179-184.

Munoz, J., Stange, D.E., Schepers, A.G., van de Wetering, M., Koo, B.K., Itzkovitz, S., Volckmann, R., Kung, K.S., Koster, J., Radulescu, S., *et al.* (2012). The Lgr5 intestinal stem cell signature: robust expression of proposed quiescent '+4' cell markers. Embo J *31*, 3079-3091.
Potten, C.S. (2004). Radiation, the ideal cytotoxic agent for studying the cell biology of tissues such as the small intestine. Radiat Res *161*, 123-136.

Potten, C.S., Booth, C., and Pritchard, D.M. (1997). The intestinal epithelial stem cell: the mucosal governor. Int J Exp Pathol *78*, 219-243.

Potten, C.S., Booth, C., Tudor, G.L., Booth, D., Brady, G., Hurley, P., Ashton, G., Clarke, R., Sakakibara, S., and Okano, H. (2003). Identification of a putative intestinal stem cell and early lineage marker; musashi-1. Differentiation *71*, 28-41.

Powell, A.E., Wang, Y., Li, Y., Poulin, E.J., Means, A.L., Washington, M.K., Higginbotham, J.N., Juchheim, A., Prasad, N., Levy, S.E., *et al.* (2012). The pan-ErbB negative regulator Lrig1 is an intestinal stem cell marker that functions as a tumor suppressor. Cell *149*, 146-158.

Qiu, W., Carson-Walter, E.B., Kuan, S.F., Zhang, L., and Yu, J. (2009a). PUMA suppresses intestinal tumorigenesis in mice. Cancer Res *69*, 4999-5006.

Qiu, W., Carson-Walter, E.B., Liu, H., Epperly, M., Greenberger, J.S., Zambetti, G.P., Zhang, L., and Yu, J. (2008). PUMA regulates intestinal progenitor cell radiosensitivity and gastrointestinal syndrome. Cell Stem Cell *2*, 576-583.

Qiu, W., Leibowitz, B., Zhang, L., and Yu, J. (2009b). Growth factors protect intestinal stem cells from radiation-induced apoptosis by suppressing PUMA through the PI3K/AKT/p53 axis. Oncogene *29*, 1622–1632.

Qiu, W., Wang, X., Buchanan, M., He, K., Sharma, R., Zhang, L., Wang, Q., and Yu, J. (2013). ADAR1 is essential for intestinal homeostasis and stem cell maintenance. Cell death & disease *4*, e599.

Qiu, W., Wang, X., Leibowitz, B., Liu, H., Barker, N., Okada, H., Oue, N., Yasui, W., Clevers, H., Schoen, R.E., *et al.* (2010). Chemoprevention by nonsteroidal anti-inflammatory drugs eliminates oncogenic intestinal stem cells via SMAC-dependent apoptosis. Proc Natl Acad Sci U S A *107*, 20027-20032.

Qiu, W., Wu, B., Wang, X., Buchanan, M.E., Regueiro, M.D., Hartman, D.J., Schoen, R.E., Yu, J., and Zhang, L. (2011). PUMA-mediated intestinal epithelial apoptosis contributes to ulcerative colitis in humans and mice. J Clin Invest *121*, 1722-1732.

Roberts, S.A., and Potten, C.S. (1994). Clonogen content of intestinal crypts: its deduction using a microcolony assay on whole mount preparations and its dependence on radiation dose. Int J Radiat Biol *65*, 477-481.

Rothenberg, M.E., Nusse, Y., Kalisky, T., Lee, J.J., Dalerba, P., Scheeren, F., Lobo, N., Kulkarni, S., Sim, S., Qian, D., *et al.* (2012). Identification of a cKit(+) colonic crypt base secretory cell that supports Lgr5(+) stem cells in mice. Gastroenterology *142*, 1195-1205 e1196.

Sangiorgi, E., and Capecchi, M.R. (2008). Bmi1 is expressed in vivo in intestinal stem cells. Nat Genet *40*, 915-920.

Sato, T., van Es, J.H., Snippert, H.J., Stange, D.E., Vries, R.G., van den Born, M., Barker, N., Shroyer, N.F., van de Wetering, M., and Clevers, H. (2011). Paneth cells constitute the niche for Lgr5 stem cells in intestinal crypts. Nature *469*, 415-418.

Sato, T., Vries, R.G., Snippert, H.J., van de Wetering, M., Barker, N., Stange, D.E., van Es, J.H., Abo, A., Kujala, P., Peters, P.J., *et al.* (2009). Single Lgr5 stem cells build crypt-villus structures in vitro without a mesenchymal niche. Nature *459*, 262-265.

Snippert, H.J., van Es, J.H., van den Born, M., Begthel, H., Stange, D.E., Barker, N., and Clevers, H. (2009). Prominin-1/CD133 marks stem cells and early progenitors in mouse small intestine. Gastroenterology *136*, 2187-2194 e2181.

Stelzner, M., Helmrath, M., Dunn, J.C., Henning, S.J., Houchen, C.W., Kuo, C., Lynch, J., Li, L., Magness, S.T., Martin, M.G., *et al.* (2012). A nomenclature for intestinal in vitro cultures. Am J Physiol Gastrointest Liver Physiol *302*, G1359-1363.

Takeda, N., Jain, R., LeBoeuf, M.R., Wang, Q., Lu, M.M., and Epstein, J.A. (2011). Interconversion between intestinal stem cell populations in distinct niches. Science *334*, 1420-1424.

Terry, N.H., and Travis, E.L. (1989). The influence of bone marrow depletion on intestinal radiation damage. Int J Radiat Oncol Biol Phys *17*, 569-573.

van Es, J.H., Sato, T., van de Wetering, M., Lyubimova, A., Nee, A.N., Gregorieff, A., Sasaki, N., Zeinstra, L., van den Born, M., Korving, J., *et al.* (2012). Dll1+ secretory progenitor cells revert to stem cells upon crypt damage. Nat Cell Biol *14*, 1099-1104.

Van Landeghem, L., Santoro, M.A., Krebs, A.E., Mah, A.T., Dehmer, J.J., Gracz, A.D., Scull, B.P., McNaughton, K., Magness, S.T., and Lund, P.K. (2012). Activation of two distinct Sox9-EGFP-expressing intestinal stem cell populations during crypt regeneration after irradiation. Am J Physiol Gastrointest Liver Physiol *302*, G1111-1132.

Wang, F., Scoville, D., He, X.C., Mahe, M., Box, A., Perry, J., Smith, N.R., Lei Nanye, N., Davies, P.S., Fuller, M.K., *et al.* (2013). Isolation and Characterization of Intestinal Stem Cells Based on Surface Marker Combinations and Colony-Formation Assay. Gastroenterology.

Wang, X., Wei, L., Cramer, J.M., Leibowitz, B.J., Judge, C., Epperly, M., Greenberger, J., Wang, F., Li, L., Stelzner, M.G., *et al.* (2015). Pharmacologically blocking p53-dependent apoptosis protects intestinal stem cells and mice from radiation. Scientific reports *5*, 8566.

Wang, Y., Wang, X., Flores, E.R., Yu, J., and Chang, S. (2016). Dysfunctional telomeres induce p53-dependent and independent apoptosis to compromise cellular proliferation and inhibit tumor formation. Aging Cell *15*, 646-660.

Wei, L., Leibowitz, B.J., Wang, X., Epperly, M., Greenberger, J., Zhang, L., and Yu, J. (2016). Inhibition of CDK4/6 protects against radiation-induced intestinal injury in mice. J Clin Invest *126*, 4076-4087.

Winton, D.J., and Ponder, B.A. (1990). Stem-cell organization in mouse small intestine. Proc Biol Sci *241*, 13-18.

Withers, H.R., and Elkind, M.M. (1969). Radiosensitivity and fractionation response of crypt cells of mouse jejunum. Radiat Res *38*, 598-613.

Wong, V.W., Stange, D.E., Page, M.E., Buczacki, S., Wabik, A., Itami, S., van de Wetering, M., Poulsom, R., Wright, N.A., Trotter, M.W., *et al.* (2012). Lrig1 controls intestinal stem-cell homeostasis by negative regulation of ErbB signalling. Nat Cell Biol *14*, 401-408.

Wu, B., Qiu, W., Wang, P., Yu, H., Cheng, T., Zambetti, G.P., Zhang, L., and Yu, J. (2007). p53 independent induction of PUMA mediates intestinal apoptosis in response to ischaemia-reperfusion. Gut *56*, 645-654.

Yan, K.S., Chia, L.A., Li, X., Ootani, A., Su, J., Lee, J.Y., Su, N., Luo, Y., Heilshorn, S.C., Amieva, M.R., *et al.* (2012). The intestinal stem cell markers Bmi1 and Lgr5 identify two functionally distinct populations. Proc Natl Acad Sci U S A *109*, 466-471.

Yu, H., Shen, H., Yuan, Y., XuFeng, R., Hu, X., Garrison, S.P., Zhang, L., Yu, J., Zambetti, G.P., and Cheng, T. (2010). Deletion of Puma protects hematopoietic stem cells and confers long-term survival in response to high-dose gamma-irradiation. Blood *115*, 3472-3480.

Yu, J. (2013). Intestinal stem cell injury and protection during cancer therapy. Transl Cancer Res *2(5):*, 384-396, doi: 310.3978/j.issn.2218-3676X.2013.3907.3903.

Zhu, L., Gibson, P., Currle, D.S., Tong, Y., Richardson, R.J., Bayazitov, I.T., Poppleton, H., Zakharenko, S., Ellison, D.W., and Gilbertson, R.J. (2009). Prominin 1 marks intestinal stem cells that are susceptible to neoplastic transformation. Nature *457*, 603-607.